Discovery and Characterization of Cooperative Ligand Binding in the Adaptive Region of Interleukin-2

Jennifer Hyde, Andrew C. Braisted, Mike Randal, and Michelle R. Arkin*

Sunesis Pharmaceuticals, 341 Oyster Point Boulevard, South San Francisco, California 94080

Received January 24, 2003

ABSTRACT: The cytokine hormone interleukin-2 (IL-2) contains a highly adaptive region that binds small, druglike molecules. The binding properties of this adaptive region have been explored using a "tethering" method that relies on the formation of a disulfide bond between the protein and small-molecule ligands. Using tethering, surface plasmon resonance (SPR), and X-ray crystallography, we have discovered that the IL-2 adaptive region contains at least two cooperative binding sites where the binding of a first ligand to one site promotes or antagonizes the binding of a second ligand to the second site. Cooperative energies of interaction of −2 kcal/mol are observed. The observation that the adaptive region contains two adjacent sites may lead to the development of tight-binding antagonists of a protein−protein interaction. Cooperative ligand binding in the adaptive region of IL-2 underscores the importance of protein dynamics in molecular recognition. The tethering approach provides a novel and general strategy for discovering such cooperative binding interactions in specific, flexible regions of protein structure.

There is a growing appreciation in drug-discovery research that proteins are dynamic systems (*1*−*3*). Computational studies have indicated that many ligand-binding sites include a dynamic region of structure that becomes organized upon ligand binding (*1*). Similarly, in several cases of active site and allosteric site binding, the structures of protein−inhibitor complexes reveal a protein surface not observed in the unbound state (see, for example, refs *4*−*10*). The binding "hot spots" at protein−protein interfaces have also been shown to contain regions of flexibility, with proteins binding to multiple protein or peptide partners through structural adaptation (*11*−*13*). The discovery of small-molecule antagonists for protein−protein systems has been especially challenging (for recent reviews, see refs *14*−*19*). New methods that are able to take advantage of protein adaptivity would therefore provide avenues for discovering drugs toward a number of different target classes.

Fragment assembly strategies have been shown to be rapid methods for identifying small-molecule leads (*20*−*23*). With this approach, weakly binding fragments (MW < 200 Da) are discovered and then linked in a second step to create a druglike ligand. Fragment assembly thus allows one to undertake a broad search of chemical space without having to make a large number of compounds. Two important challenges of fragment assembly are identifying weakly binding fragments and determining how to link these fragments productively. Productive linking implies that the free energy of binding for the linked molecule is approximately the sum of the free energies of binding for the fragments themselves. However, fragment discovery methods that can identify cooperatively binding molecules would be preferred, since cooperativity offers the opportunity to further augment the affinity of the linked compound (*24*).

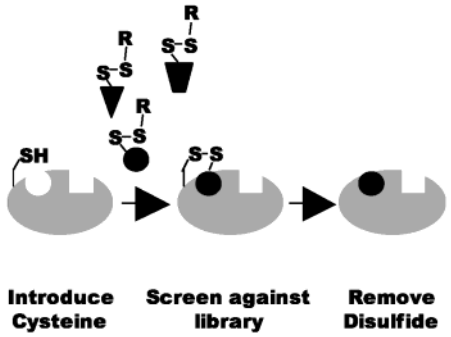

FIGURE 1: Tethering experiment. A protein is engineered to contain a single cysteine residue near a target site for small-molecule binding (left). The protein is then interrogated with a library of disulfide-containing fragments under conditions that facilitate thiol−disulfide exchange. Compounds that both bind the protein and form a disulfide bond are selected (center). Finally, the disulfide is removed from the fragment, and the fragment is characterized for noncovalent binding to the wild-type protein (right).

We have used a fragment discovery method called tethering (Figure 1) to screen for small-molecule ligands that bind in an adaptive region of protein structure. Tethering addresses the issue of identifying weak binders by capturing fragments at specific sites in a protein with a covalent bond (*22*, *23*). The target protein is engineered to contain a single, reactive cysteine residue near a binding site. This protein is then probed with a library of disulfide-containing fragments under conditions that facilitate thiol−disulfide exchange. After equilibrium has been reached, the reaction mixture is analyzed by mass spectrometry, and compounds that both bind to the protein and form a disulfide bond with the cysteine residue are identified. The site-directed nature of the tethering approach makes it well-suited to searching for new ligand-binding sites in the adaptive region of proteins. Here, we extend the method to focus on ligands that bind cooperatively to such regions.

* To whom correspondence should be addressed. Telephone: (650) 266-3603. E-mail: mra@sunesis.com.

10.1021/bi034138g CCC: $25.00
Published on Web 05/06/2003

Chart 1: Structure of Compound **1**

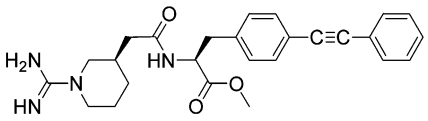

Recent work with the T-cell cytokine interleukin-2 (IL-2) suggests that small, nonpeptidyl molecules can target the dynamic regions at a protein−protein interface. IL-2, which stimulates the proliferation of activated T-cells by signaling through the trimeric IL-2 receptor [IL-2R (*25*)], is a well-validated drug target for immunological disease (*26*−*29*). Structural studies of IL-2 have shown that the binding interface for the α-chain of IL-2R (IL-2Rα) (*30*−*33*) contains both rigid and flexible portions of protein structure (*34*). Small, organic molecules that bind to IL-2 at the IL-2Rα site take advantage of this flexibility, revealing a binding site conformation not observed in the X-ray structures of unliganded IL-2. Compound **1**, discovered at Hoffman-LaRoche (Chart 1) (*35*), was the first small-molecule inhibitor of IL-2 to be characterized by X-ray crystallography [Figure 2 (*34*)]. The dynamic region of IL-2 revealed by this structure includes the hydrophobic portion of the binding site, characterized by surface residues F42, R38, and L72, and extends through the two loops (amino acids 30−33 and 73−81) adjacent to the binding site of **1**. The observations that organic molecules preferentially bind to the adaptive region of IL-2 and that compound **1** does not fill the adaptive area led us to consider whether there are additional binding sites for small molecules within the hydrophobic, flexible region of IL-2.

We screened for additional binding interactions outside the binding site of **1** by tethering in the presence of a saturating concentration of compound **1**. We expected that **1** would block the known binding site and also alter the structure of IL-2 relative to its unbound conformations. We find that compound **1** has a dramatic effect on the selection of fragments by tethering. The tethering of some fragments was synergistic with the binding of **1**, and we set out to understand the mechanism and energetics of this cooperativity. The data indicate that cobinding of **1** increases the affinity of fragments by as much as −2 kcal/mol. These results highlight the importance of protein adaptability in molecular recognition. Tethering in the presence of known ligands provides a novel approach for discovering new binding sites and for characterizing their small-molecule binding properties.

EXPERIMENTAL PROCEDURES

Preparation of Proteins and Compounds. IL-2 and mutants were prepared as described previously (*34*). Synthesis of the disulfide library has been described previously (*22*). Selected hits were also prepared as nonexchangeable capped analogues by converting the same functional group used to install the disulfide linker (either an amine or a carboxylic acid) to a neutral amide linker through condensation with either 3-methoxypropionic acid or 2-methoxyethylamine.

Primary Tether Screening. A single, purified IL-2 cysteine mutant (N30C, Y31C, or N33C) (*34*) at 10 μM in 100 mM HEPES buffer (pH 7.4) was combined with 4 mM βME and 2 mM total disulfide-containing compounds (10 compounds at 200 μM each) at a final DMSO concentration of 2%. Each mixture was tested in the presence and absence of 50 μM **1**. Mixtures were allowed to come to equilibrium (2−8 h) at room temperature and then were analyzed by liquid chromatography−mass spectrometry (LC−MS) as previously described (*34*). Compounds which modified the cysteine mutant of IL-2 by more than 30% were retested as single compounds.

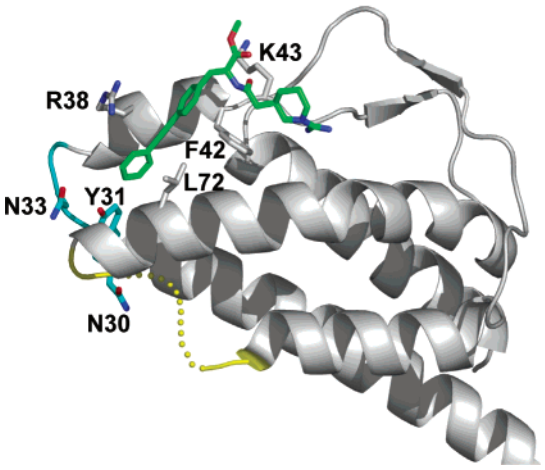

FIGURE 2: X-ray crystal structure of compound **1** bound to IL-2 (PDB entry 1M48). IL-2 is shown as a ribbon, with residues discussed in the text shown in stick representation. The adaptive region of the compound **1** binding site (see the text) includes residues R38, F42, and L72 and extends through the two loops (light blue and yellow) adjacent to these residues. The loop connecting residues 78−83 is not observed in the electron density and is denoted with dots in the ribbon diagram. Residues used for tethering experiments (N30, Y31, N33, and K43) are also shown. Carbon atoms are colored gray or light blue, nitrogen atoms blue, oxygen atoms red, and sulfur atoms yellow. Structures were rendered in Pymol (DeLano Scientific, San Carlos, CA).

Compound Titrations. The concentration of a disulfide-containing fragment required for labeling an IL-2 cysteine mutant by 50% (50% dose−response value, DR_{50}) was determined by monitoring the percentage of the fragment−protein conjugate as a function of compound concentration. Dose−response titrations were performed with 10 μM IL-2 mutant, 4 mM βME, and seven concentrations of the fragment disulfide (from 62 μM to 4 mM) at room temperature. Two types of titrations were compared. First, fragment disulfides were added to a single mutant of IL-2 (Y31C or N33C) in the absence of **1**. Second, fragment disulfides were added to these mutants in the presence of 50 μM compound **1**. Mixtures were allowed to come to equilibrium (2−8 h) at room temperature and then were analyzed by LC−MS as previously described (*34*). Data were plotted (Kaleidagraph, Synergy Software) and fit by nonlinear regression to obtain the DR_{50}.

Titrations with Y31C/K43C-IL-2. Two types of dose−response titrations were performed with a double mutant (Y31C/K43C). In the first type of titration, fragment disulfides (62−4000 μM) were added to the double mutant of IL-2 (1 μM) in the presence of 4 mM βME and a variant of **1** (5 μM) containing a disulfide (**1t**). In the second type of experiment, titrations were performed by adding **1t** in the presence and absence of tethering fragments. Seven concentrations of **1t** (from 700 nM to 500 μM) were mixed with 1 μM Y31C/K43C, 1 mM fragment disulfide, and 4 mM βME, in a buffer of 100 mM HEPES (pH 7.4).

Because a low concentration of IL-2 was used, the double mutant titrations were analyzed with an LC−MS system more sensitive than that used previously. These experiments utilized an HP 1100 chromatography system (Agilent, Palo Alto, CA), an HTS PAL autosampler (LEAP Technology, Carrboro, NC), and a hybrid quadrupole time-of-flight QSTAR Pulsar I mass spectrometer (PE Sciex Instruments, Toronto, ON) outfitted with a MicroIonSpray electrospray ionization source. Chromatography was conducted on a Phenomenex Jupiter C5 column (50 mm × 2.0 mm) with a gradient from 10 to 90% acetonitrile in water containing 1% formic acid over the course of 1.9 min. Chromatography was performed at a flow rate of 750 μL/min, and a small amount of eluate was then passed into the mass spectrometer at a rate of 25 μL/min. Mass spectrometry was performed in positive ion mode, scanning the range of *m*/*z* 900−2000. Settings were controlled by the Analyst computer software package (PE Sciex Instruments).

Surface Plasmon Resonance. Wild-type IL-2 and K43C-IL-2 modified with **1t** were immobilized on a CM5 chip (Biacore, Uppsala, Sweden) using standard amine coupling. Between 4000 and 8000 RU of IL-2 was immobilized; 4000 RU of protein tyrosine phosphatase (PTP-1B) was immobilized on the same chip as a control for nonspecific binding. No nonspecific binding was detected for **1** or for any of the fragments that were tested. Eight concentrations of compound (from 4 to 500 μM) in phosphate-buffered saline (PBS) with 0.05% azide and 1% DMSO were passed over the IL-2/PTP-1B-labeled chip at a rate of 40 μL/min at 25 °C. The stoichiometry of binding was estimated with the equation

$$\text{stoichiometry} = (\text{RU}_{\text{ligand}}/\text{MW}_{\text{ligand}})(\text{MW}_{\text{protein}}/\text{RU}_{\text{protein}})$$

where MW is the molecular mass. The dissociation constant ($K_{d,SPR}$) for each compound was determined by plotting the RU at the plateau of the binding curve versus the compound concentration; data were fit by nonlinear regression. $K_{d,SPR}$ values were determined in the presence and absence of 50 μM **1** in the sample buffer.

X-ray Crystallography. The carboline fragment (**7t**) was tethered to the Y31C mutant of IL-2 by the following procedure. Y31C-IL-2 was expressed and refolded; under the refolding conditions, Y31C was found to be a mixed disulfide with cystamine. The Y31C residue was reduced by treating 0.5 mg of Y31C-IL-2 with 10 mM βME for 4 h at room temperature. βME was removed by desalting (NAP5, Pharmacia, Uppsala, Sweden), and the protein solution was concentrated to 100 μM protein using an Ultrafree centrifugation filter (Millipore, Bedford, MA). Then 500 μM **7t**, 100 μM βME, and 100 μM compound **1** were incubated with the protein overnight at 4 °C. The fragment−protein conjugate was then separated from βME and **1** by desalting (NAP5, Pharmacia). Monitoring by LC−MS (*34*) showed that 100% of Y31C-IL-2 was labeled with compound **7t**.

Crystals were grown by standard hanging-drop vapor diffusion methods from a reservoir of 30% PEG 8K and 0.2 M $(NH_4)_2SO_4$. Prior to data collection, crystals were transferred to a reservoir solution supplemented with 20% glycerol. Diffraction data were collected at −180 °C using an R-AXIS-IV (Rigaku) detector mounted on an RU-3R generator and processed with D*TREK (*36*) (Table 1). The structures were determined by molecular replacement using AMORE (*37*) and refined with REFMAC5 (*37*). The protein models were adjusted using O (*38*) and ligand models constructed in INSIGHT-II (Molecular Simulations, Waltham, MA). Solvent molecules were placed automatically using ARP_WATERS (*37*), and refinement continued until no interpretable features remained in $F_o - F_c$ difference maps. The final model is summarized in Table 1.

Table 1: Crystallographic Data

space group	$P2_12_12$
cell dimensions (Å)	$a = 49.16$
	$b = 85.35$
	$c = 31.71$
no. of molecules per asymmetric unit	1
resolution (Å)	10−2.2
no. of unique reflections	7042
completeness[a] (%)	98.2 (96.9)
$R_{sym}(I)$[b] (%)	6.9 (25.3)
I/σ	17.5 (5.5)
R_{cryst}[c] (%)	22.8
R_{free}[d] (%)	27.7 (342)
average *B* factor (Å^2)	
protein	29.9
solvent	37.2
ligand	40.5

[a] Values in parentheses are for the highest-resolution bin. [b] $R_{sym}(I) = \sum_{hkl}|I_{hkl} - \langle I_{hkl}\rangle|/\sum_{hkl}I_{hkl}$, where I_{hkl} is the intensity of reflection *hkl*. [c] $R_{cryst} = \sum_{hkl}||F_{obs}| - |F_{calc}||/|F_{obs}|$, where F_{obs} and F_{calc} are the observed and calculated structure factors, respectively, for the data used in refinement. [d] $R_{free} = \sum_{hkl}||F_{obs}| - |F_{calc}||/|F_{obs}|$, where F_{obs} and F_{calc} are the observed and calculated structure factors, respectively, for data omitted from refinement (number of included reflections in parentheses).

RESULTS AND DISCUSSION

Tethering in the Adaptive Region of IL-2. Analysis of the costructure of **1** and IL-2 (Figure 2) suggested that residues N30, Y31, and N33 would be well-suited to accessing the adaptive region adjacent to the binding site of compound **1**. Previous studies had shown that cysteine mutations at these sites had no effect on the overall conformation or activity of IL-2, and furthermore showed that these residues select large numbers of fragments from our in-house fragment disulfide library (*34*). The cysteine mutants were screened against the most active subset of this library at 4 mM βME in both the absence and presence of a saturating concentration of **1**. Table 2 describes the results from screening at a single concentration of the disulfide library. In all, approximately 7000 compound/protein pairs were screened, and 132 fragments labeled the IL-2 mutants by at least 30% under one of the screening conditions. Of these selected compounds, 31 fragments were unaffected by the binding of **1**, 57 fragments showed at least 2-fold decreases in the level of protein conjugation, and 44 fragments showed at least 2-fold increases in the level of protein conjugation in the presence of **1**. In fact, the effect of **1** was usually more dramatic; 95% of inhibited compounds showed decreases of more than 4-fold, and 68% of augmented compounds showed increases of more than 4-fold. An example of an augmented compound is shown in Figure 3. These results demonstrate that the selection of specific fragments is tightly coupled to the presence of **1**.

Quantification of Tethering Cooperativity. The binding augmentation observed in the initial tethering screen was

Table 2: Summary of the Tether Screen in the Presence and Absence of Compound **1**

mutant	no. of compounds screened[a]	no effect[b]	inhibited[c]	augmented[d]
N30C	800	0	5	6
Y31C	4156	21	32	27
N33C	2084	10	20	11
total	7040	31	57	44

[a] Compounds in the tethering library screened in pools of 10 compounds, as described in Experimental Procedures. Conditions: 2 mM compound pool, 10 μM IL-2 mutant, and 4 mM βME. [b] Number of compounds for which the percent of protein conjugated with the tethering fragment was less than 2-fold different in the presence and absence of **1**. [c] Number of compounds for which the percent of protein conjugated with the tethering fragment was more than 2-fold greater in the *absence* of **1** than in its presence. [d] Number of compounds for which the percent of protein conjugated with the tethering fragment was more than 2-fold greater in the *presence* of **1** than in its absence.

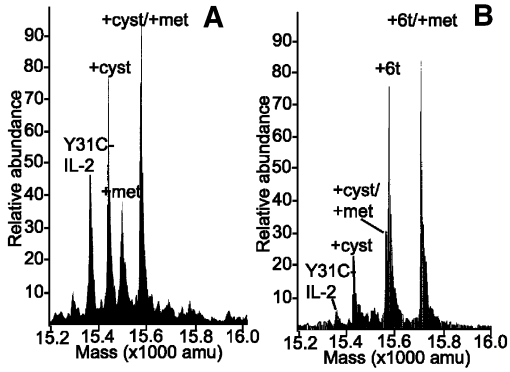

FIGURE 3: Mass spectrometry data from the tethering screen. (A) Deconvoluted, neutral scale mass spectrum of Y31C-IL-2 in the presence of a pool of 10 disulfide-containing fragments. (B) Deconvoluted, neutral scale mass spectrum of the same mutant and fragment pool in the presence of 50 μM compound **1**. Peaks in the spectra are labeled as follows: Y31C-IL-2, mass of the unmodified protein (15 358 Da); +cyst, mass of the protein modified with cystamine at Y31C (15 432 Da); +met, mass of the unmodified protein with an N-terminal methionine (15 488 Da); +cyst/+met, mass of the protein containing an N-terminal methionine and labeled with cystamine at Y31C (15 565 Da); +6t, mass of Y31C-IL-2 modified with compound **6t** (15 577 Da); and +6t/+met, mass of Y31C-IL-2 containing an N-terminal methionine and modified with compound **6t** (15 708 Da). The yield of the fragment−protein conjugate is negligible in the absence of **1** (A) and 84% in the presence of 50 μM **1** (B).

striking, and we therefore focused our effort on understanding the mechanism of the observed cooperativity between fragments and compound **1**. Compounds chosen for further analysis are shown in Figure 4. These fragments were characterized by a dose−response curve in which the percentage of the protein−fragment conjugate is plotted as a function of the fragment concentration (sample data shown in Figure 5). The dose−response curve yields a DR_{50}, the concentration of the compound at which 50% of the protein is in the conjugated form at 4 mM βME. The DR_{50} is an apparent dissociation constant, and includes contributions from thiol−disulfide equilibria as well as noncovalent interactions between the compound and protein. Analogous to a dissociation constant, a small value for DR_{50} denotes a strong tether conjugate.

The results of dose−response data are shown in Table 3, where the designation "t" indicates that the fragment is functionalized with a disulfide for tethering. In each case,

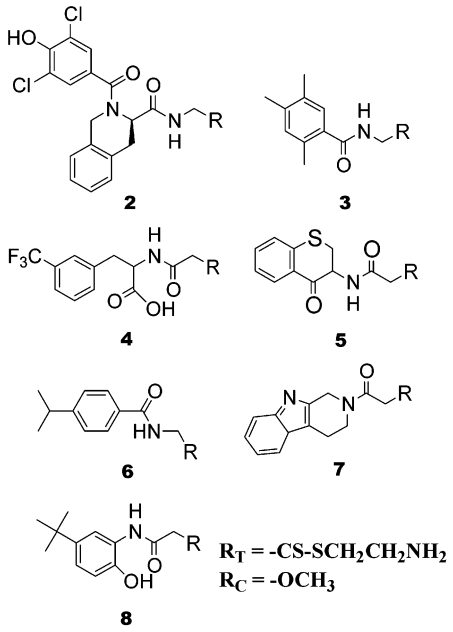

FIGURE 4: Chemical structures of fragments selected for further study. Compounds containing CS-$SCH_2CH_2NH_2$ as the R_t group have an exchangeable disulfide for tethering. Compounds containing OCH_3 as the R_c group are chemically inert and are used to measure the level of noncovalent binding to IL-2. In the text, compounds containing R_t are denoted with a "t" and those containing R_c are denoted with a "c".

compounds identified as being cooperative with **1** in the primary screen show decreased DR_{50} values when measured in the presence of **1** compared to the DR_{50} values measured without **1** present. Analogously, the inhibited compound yields an increased DR_{50} value when **1** is present.

The effects of bound compound **1** on both the augmentation and inhibition of tethered compounds are impressive. For example, tethering of compound **6t** to the Y31C mutant of IL-2 (Y31C-IL-2) is 30-fold more efficient in the presence of **1** than in its absence (DR_{50} = 90 and 3000 μM with **1** and without **1**, respectively). Similarly, compound **8t** tethers to Y31C-IL-2 with moderate efficiency in the absence of **1**, but is completely inhibited in the presence of **1** (DR_{50} > 4000 μM with **1** and DR_{50} = 750 μM without **1**). Dose−response assays consistently support the screening data and demonstrate that there can be large differences in the apparent binding of tethering hits depending on whether compound **1** is also bound.

Dose−Response Curves with the Double Mutant. To further characterize cooperative binding, we prepared a tethering experiment in which both compound **1** and a fragment could be simultaneously tethered to IL-2. This experiment had two goals. First, it was important to evaluate if the apparent cooperativity between **1** and a tethered fragment resulted from simultaneous binding of both molecules. Second, we wanted to determine whether the observed cooperativity was reciprocal, i.e., whether compound **1** exhibited altered binding in the presence of fragments. These two goals are readily accomplished using a form of **1** that can be tethered to IL-2, because binding to IL-2 can then be directly assessed by mass spectrometry.

Accordingly, an analogue of compound **1** was synthesized to contain a disulfide linker. Modeling based on the cocrystal structure of **1** bound to IL-2 (Figure 2) indicated that

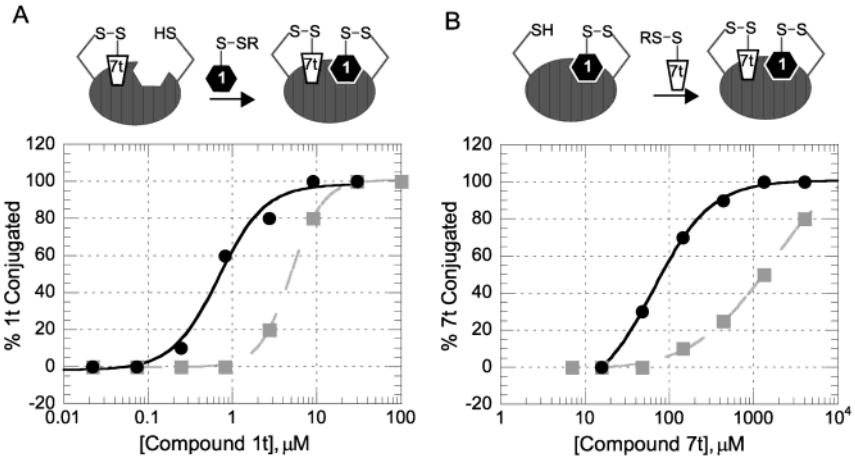

FIGURE 5: Characterization of compound **7t** by tethering to the Y31C/K43C mutant of IL-2. (A) Scheme depicting experiment and data showing the percent of IL-2 conjugated to **1t** as a function of the concentration of **1t** in the presence (black) and absence (gray) of 1 mM **7t**. Half-maximal tethering occurs at 1 and 5 μM, respectively, indicating a 5-fold enhancement. (B) Scheme depicting experiment and data showing the percent of IL-2 conjugated to **7t** as a function of the concentration of **7t** in the presence (black) or absence (gray) of 5 μM **1t**. Half-maximal tethering occurs at 80 and 1000 μM, respectively, indicating a 12-fold enhancement.

Table 3: Tether Screening and Characterization

			N33C-IL-2 or Y31C-IL-2[a]			Y31C/K43C-IL-2[b]		
tether fragment[c]	cysteine[d]	hit class[e]	DR_{50} (μM) without **1**[f]	DR_{50} (μM) with **1**[g]	fold increase[h]	DR_{50} (μM) without **1t**[i]	DR_{50} (μM) with **1t**[j]	fold increase[k]
2t	N33	equal	500	250	2.0			
3t	Y31	equal	250	140	1.8			
4t	Y31	augmented	480	270	1.8	440	130	3.4
5t	Y31	augmented	>4000	210	>20.0	>4000	200	>20.0
6t	Y31	augmented	3000	90	30.0	>4000	130	>30.0
7t	Y31	augmented	1180	140	8.0	1000	80	12.0
8t	Y31	inhibited	750	>4000	<0.2			

[a] N33C mutant of IL-2 used for measuring dose−response curves for **2t**; Y31C mutant of IL-2 used for **3t**−**8t**. [b] Y31C/K43C double mutant of IL-2 used for measuring dose−response curves. [c] From Figure 4. [d] Cysteine residue at which fragment was identified. [e] Fragment classified by primary screening as defined in the text and Table 2. [f] DR_{50} value, defined as the concentration of fragment needed to label IL-2 by 50%, measured under the following conditions: 10 μM IL-2 mutant, 62−4000 μM tethering fragment, and 4 mM βME. [g] DR_{50} value measured under the following conditions: 10 μM IL-2 mutant, 62−4000 μM tethering fragment, 4 mM βME, and 50 μM compound **1**. [h] Ratio of DR_{50} values in the absence and presence of compound **1**. [i] DR_{50} value measured under the following conditions: 1 μM IL-2 mutant, 62−4000 μM tethering fragment, and 4 mM βME. [j] DR_{50} value measured under the following conditions: 1 μM IL-2 mutant, 62−4000 μM tethering fragment, 4 mM βME, and 5 μM compound **1t**. [k] Ratio of DR_{50} values in the absence and presence of **1t**. For all measurements, $n \geq 2$.

Scheme 2: Structure of Compound **1t**

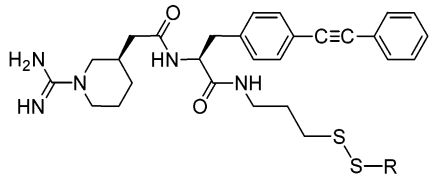

compound **1** could be tethered to a K43C mutant of IL-2 if the compound contained a disulfide linker with a three-methylene spacer (Chart 2). The disulfide-containing analogue (**1t**) was tested for the ability to label the Y31C/K43C double mutant of IL-2 (Y31C/K43C-IL-2). Tethering of **1t** to Y31C/K43C-IL-2 consistently gave a DR_{50} value of 5−6 μM under the experimental conditions (Figure 5A). Furthermore, the complex between Y31C/K43C-IL-2 and **1t** no longer interacted with IL-2Rα (data not shown), suggesting that the tethered compound **1t** bound to IL-2 at the same binding site as did compound **1** itself.

Table 3 summarizes the dose−response data for cooperative fragments **4t**−**7t** binding to Y31C/K43C-IL-2 in the presence and absence of **1t** at 4 mM βME. The mass spectrometry data clearly distinguish the unmodified protein from all three tethered species (Y31C/K43C-IL-2 conjugated to fragment, Y31C/K43C-IL-2 conjugated to **1t**, and Y31C/K43C-IL-2 conjugated to both compounds simultaneously; data not shown). For fragments **4t**−**7t**, the dose−response curves in the presence of **1t** agree closely with the data obtained using Y31C-IL-2 and noncovalently bound **1**. In the case of compound **7t**, for example, the dose−response curves indicate an 8- and 12-fold enhancement in tethering in the presence of **1** and **1t**, respectively. Throughout the dose−response titrations, **1t** remained bound to IL-2. These data indicate that cooperative tethering (decrease in DR_{50}) requires the cobinding of **1**.

Tethering experiments using Y31C/K43C-IL-2 also allowed us to test whether the tethering of **7t** and **8t** at Y31C influenced the tethering of **1t** at K43C.[1] Figure 5 shows the results of dose−response measurements of compounds **7t** and **1t** bound to Y31C/K43C-IL-2. As described above, **7t** tethers at 12-fold lower concentrations when **1t** is covalently tethered (Figure 5B). Conversely, **1t** conjugates to Y31C/

[1] Fragment **7t** was chosen because it can be tethered to Y31C-IL-2 in the absence of **1**. The other highly cooperative fragments, **5t** and **6t**, do not significantly label protein in the absence of **1** or **1t**.

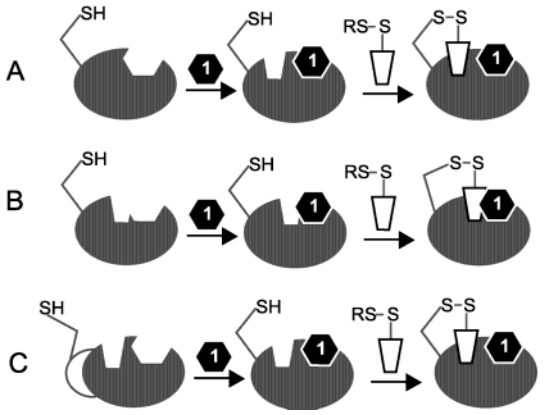

FIGURE 6: Possible mechanisms of cooperative binding observed by tethering. (A) The conformation for the second site is altered by the binding of compound **1**, augmenting binding of the second ligand. (B) A direct interaction between the two ligands increases the binding affinity for the fragment. (C) The orientation of the cysteine residue is altered by the binding of compound **1**, allowing tethering of the second ligand.

K43C-IL-2 at 5-fold lower concentrations when **7t** is simultaneously tethered (Figure 5A; $DR_{50} = 5$ μM in the absence and 1 μM in the presence of **7t**). The DR_{50} value of 1 μM for compound **1t** in the presence of **7t** represents a lower limit, since 1 μM protein was used in the tethering assay. These experiments demonstrate that **7t** and **1t** bind in a mutually cooperative fashion.

Analogously, the competitive fragment **8t** and **1t** are mutually competitive. The fragment **8t** shows a greater than 5-fold increase in DR_{50} in the presence of **1** (Table 3). Conversely, **1t** shows a 10-fold increase in DR_{50} in the presence of **8t** ($DR_{50} = 6$ μM in the absence and 60 μM in the presence of 1 mM **8t**; data not shown). This result indicates that **8t** and **1t** are competing either for the same protein contacts or for mutually exclusive binding conformations.

Noncovalent Binding of Competitive and Cooperative Compounds. The cooperativity observed in the tethering experiments suggests that the binding of **1** changes the protein conformation at a second small-molecule binding site. From the tethering data alone, there are three potential mechanisms for this observed synergy (Figure 6). Positive cooperativity could be caused by improvements in the interactions of the fragment with the protein (Figure 6A) or through direct interactions between the fragment and compound **1** (Figure 6B). Alternatively, binding of **1** could alter the conformation of the flexible loop containing the cysteine residue, allowing an already bound fragment to be captured by tethering (Figure 6C). To distinguish these mechanisms, surface plasmon resonance (SPR) was used to measure the extent of noncovalent binding of fragments to wild-type IL-2 in the presence and absence of **1**. If cooperativity were due to the orientation of Y31C (Figure 6C), then no cooperativity should be observed for noncovalently bound ligands.

For these SPR studies, fragments were prepared with a chemically inert, methyl ether "cap" in place of the disulfide tether (Figure 4). Wild-type IL-2 was then immobilized to the surface of an SPR chip, and increasing concentrations of the capped fragment were passed over the IL-2-modified chip in the presence or absence of a constant, saturating concentration of **1**. Binding of fragments to IL-2 was monitored at the equilibrium plateau and plotted as a function of concentration to yield a dose−response curve (sample data shown in Figure 7). The dissociation constants ($K_{d,SPR}$) calculated from SPR dose−response curves are given in Table 4 for five representative fragments. In all cases, fragments showed low-stoichiometry binding to IL-2 in both the presence and absence of **1**; when fragments were sufficiently soluble to reach binding saturation, they were found to bind to immobilized IL-2 with a binding stoichiometry of 1:1.

Table 4: Surface Plasmon Resonance Assay for Measuring the Level of Fragment Binding

tether selectant[a]	hit class[b]	$K_{d,SPR}$ (IL-2) (μM)[c]	$K_{d,SPR}$ (IL-2 and **1**) (μM)[d]	$K_{d,SPR}$ (K43C-IL-2 and **1t**) (μM)[e]
2c	equal	50	75	
5c	augmented	inactive	200	
6c	augmented	inactive	110	210
7c	augmented	inactive	230	250
8c	inhibited	500	inactive	

[a] From Figure 4. [b] Fragment classified by primary screening data as defined in the text and Table 2. [c] $K_{d,SPR}$ value for the fragment binding to wild-type IL-2. [d] $K_{d,SPR}$ value for the fragment binding to wild-type IL-2 in the presence of 50 μM **1** ($n \geq 2$). [e] $K_{d,SPR}$ value for the fragment binding to the K43C mutant of IL-2 modified 100% with **1t**.

SPR data confirm the tethering results. Each fragment whose binding is augmented in the presence of **1** when tethered also shows augmented binding in the noncovalent assay. For example, the three most strongly cooperative tethering hits, compounds **5c**−**7c**, show no binding to wild-type IL-2 by SPR. In the presence of **1**, however, these fragments demonstrate strong binding, with $K_{d,SPR}$ values of 200, 110, and 230 μM, respectively.[2] Similarly, the competitive compound **8c** exhibits a $K_{d,SPR}$ of 500 μM in the absence of bound **1**, but undetectable binding in the presence of **1**. Compound **2**, which was unaffected by the binding of **1** in the tether assay, is also unaffected by the presence of **1** in the SPR experiment ($K_{d,SPR} = 75$ and 50 μM in the presence and absence of **1**, respectively). In this case, tethering is surprisingly weak, given the strong, noncovalent affinity of **2c** shown by SPR. This discrepancy suggests that the binding observed by tethering is limited by a suboptimal length or conformation of the linker connecting the compound to the protein. The observation that binding to wild-type IL-2 is augmented for **5c**−**7c** and weakened for **8c** indicates that these fragments bind cooperatively or competitively with **1** on the basis of altered noncovalent interactions with IL-2.

To ensure that compound **1** was indeed bound throughout the SPR experiment, we labeled an SPR surface with a K43C mutant of IL-2 (K43C-IL-2) that had been fully labeled with the disulfide analogue **1t**. Noncovalent binding of **6c** and **7c** to this protein was compared to the fragment's binding to wild-type IL-2 (Table 4). Again, **6c** and **7c** exhibited no binding to immobilized wild-type IL-2; however, both exhibited strong binding to the **1t**-labeled K43C mutant. The values of $K_{d,SPR}$ for **6c** and **7c** agree with the values obtained when **1** was added noncovalently to the wild-type protein. These results demonstrate that **1** remains bound to wild-type

[2] The apparent dissociation constants observed in the SPR and tethering experiments are not expected to be the same, since DR_{50} values are dependent on the concentration of reductant (βME).

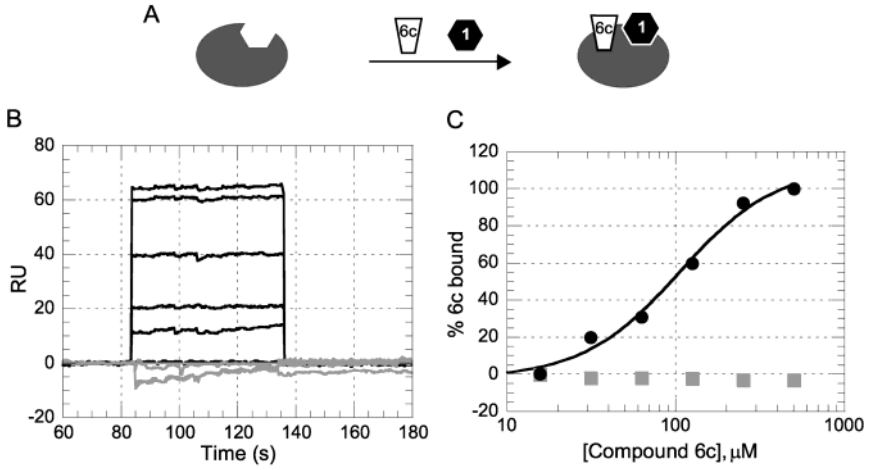

FIGURE 7: Characterization of cooperative fragments by SPR. (A) Experimental scheme for the SPR experiment. The fragment, with or without compound **1**, is passed over a chip containing immobilized IL-2. (B) Plot of bound **6c** in resonance units (RU) as a function of time. Binding profiles for six concentratons of **6c** are shown in the presence (black) and absence (gray) of 50 μM **1**. (C) Data from panel B, plotted as the percent of **6c** bound vs the concentration of **6c** in the presence (black) or absence (gray) of 50 μM **1**. $K_{d,SPR}$ = 110 μM for **6c** binding in the presence of **1**, and $K_{d,SPR}$ is unmeasurable in the absence of **1**.

IL-2 in the SPR experiment and further emphasize that the cobinding of **1** (or **1t**) has a marked cooperative effect on the binding of fragments **6c** and **7c**.

The SPR experiment is complementary to the tethering assay, and these two binding measurements have different assets and liabilities. On one hand, SPR is a more direct measurement of noncovalent binding interactions than tethering, which relies on a reversible covalent bond for detection. On the other hand, tethering permits identification of very weakly bound fragments, such as **6** and **7**, whose noncovalent binding cannot be detected by SPR in the absence of cobound **1** (Tables 3 and 4). Tethering also allows quantification of the amount of each compound bound to IL-2 throughout the titration experiment. It is therefore possible to measure the extent of competitive binding between two compounds. In contrast, since SPR measures the total mass bound to protein, it is difficult to measure the extent of competitive binding between two species of similar mass, such at **1** and **8c**.

Energetic Consequences of Cooperativity. In principle, the free energy of cooperative binding between **1** and fragments **4t**−**7t** can be obtained by comparing the tethering DR_{50} curves (*39*). However, changes in tethering (and thus DR_{50}) can be attributed to changes in molecular recognition and/or changes in the tethering reaction itself. The cooperative free energy of tethering ($\Delta\Delta G_{tether}$) can be described by the equations

$$\Delta\Delta G_{tether} = RT \ln(DR_{50,+1}/DR_{50,-1}) \quad (1)$$

$$\Delta\Delta G_{tether} = \Delta\Delta G_{noncov} + \Delta\Delta G_{thiol} + \Delta\Delta G_{linker} \quad (2)$$

where $DR_{50,+1}$ and $DR_{50,-1}$ are the DR_{50} values for tethering in the presence and absence of **1**, respectively, R is the gas constant, T is the temperature, $\Delta\Delta G_{noncov}$ describes the changes in noncovalent interactions between the protein and fragment, $\Delta\Delta G_{thiol}$ describes the energetics of thiol−disulfide exchange, and $\Delta\Delta G_{linker}$ accounts for changes in the steric constraints of the disulfide linker connecting the protein and fragment. From tethering dose−response curves, the 8−12-fold change in the DR_{50} for fragment **7t** in the presence of **1** or **1t** indicates a $\Delta\Delta G_{tether}$ of approximately −1.2 to −1.5 kcal/mol. In the case of fragment **6t**, the observed cooperativity in tethering corresponds to a $\Delta\Delta G_{tether}$ of approximately −2.1 kcal/mol. DR_{50} measurements made in the presence or absence of **1** use very similar conditions, thus reducing the importance of $\Delta\Delta G_{thiol}$; however, tethering experiments alone may not distinguish between the effects of $\Delta\Delta G_{noncov}$ and $\Delta\Delta G_{linker}$.

The effects of $\Delta\Delta G_{noncov}$ and $\Delta\Delta G_{linker}$ can be separated by comparing tethering measurements to SPR experiments. Because the weakly binding fragments could not be detected in the absence of **1**, however, it is possible only to state a lower limit for the cooperative free energy from the SPR experiment. For fragments **5c**−**7c**, this lower limit is approximately −1.4 kcal/mol, using an equation similar to eq 1 and assuming $K_{d,spr} > 2$ mM in the absence of **1**. SPR data thus provide values for cooperative free energies of binding that are similar to the free energies obtained from tethering, indicating that $\Delta\Delta G_{linker}$ is small in the tethering experiments and that cooperativity arises primarily from improvements in noncovalent binding affinity. Both tethering and SPR data show that the small-molecule binding sites in the adaptive region of IL-2 are tightly coupled, with cooperative free energies of binding as large as −2 kcal/mol.

*Structural Characterization of **7t**.* Y31C-IL-2 was modified with **7t**, and the structure of the tethered complex was determined by X-ray crystallography (Figure 8A, PDB entry 1NBP). The structure of **7t** is clearly defined by the electron density. The tethered compound is several angstroms from the IL-2Rα (and compound **1**) binding site; in fact, it is found close to the binding site for the β-chain of the IL-2 receptor (IL-2Rβ) (*31*, *33*). The carboline moiety of **7t** forms a shallow cup shape, and closely contacts residue L70 on the concave face and residues F78 and L80 on the convex face. The carboline is also in van der Waals contact with residues M23, I24, G27, I28, P82, and L85; in all, 99% of the surface area of the carboline is buried in the structure [DIFFAREA (*37*)].

The adaptive region of IL-2 wraps around the surface of the carboline, enclosing the tethered compound in a highly complementary, hydrophobic binding envelope. Interestingly,

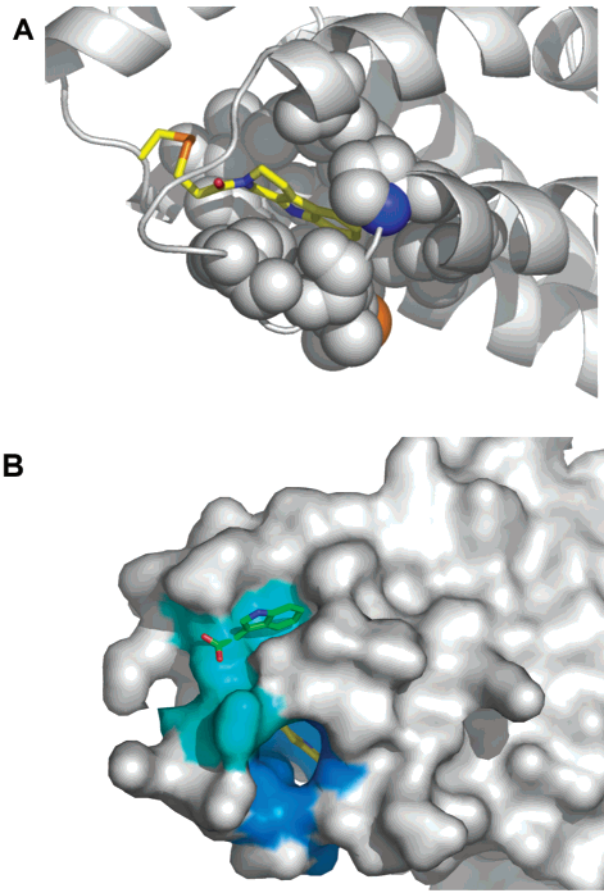

FIGURE 8: X-ray crystal structure of **7t** bound to Y31C-IL-2. (A) View of the **7t** binding site on Y31C-IL-2. Fragment **7t** is shown in stick representation; carbon atoms are shown in yellow, oxygens in red, and nitrogens in blue. IL-2 is shown as a ribbon diagram; the side chains of residues in van der Waals contact with **7t** are shown as spheres, with carbon atoms in white, oxygens in red, nitrogens in blue, and sulfurs in orange. (B) X-ray structure of **7t** bound to Y31C-IL-2 with the structure of indole glyoxylate (1M4A) superimposed on its binding site. IL-2 is shown in white surface representation. Residues in van der Waals contact with the indole glyoxylate are shown in light blue; residues in contact with **7t** are shown in dark blue. Indole glyoxylate (green) and **7t** (yellow) are shown in stick representation, with oxygen atoms colored red and nitrogens colored blue. These images were rendered in Pymol (DeLano Scientific).

several of the residues surrounding **7t** are found on a loop (residues 73−81), which is disordered or partially ordered in several of the X-ray structures of IL-2 [PDB entries 1M47, 1M48, 1M4A, 1M4B, and 1M4C (*34*)]. In the cases for which electron density is observed for residues 73−81 (*40*, *41*), the hydrophobic residues in the loop are found to be well-packed against the protein, and no binding site for **7t** exists. Thus, the binding site for the carboline is highly flexible and appears to be organized by the binding of **7t**. Compound **1** is not present in the determined structure, so we cannot rule out the possibility that **7t** has a different binding site in the presence of **1**. Nevertheless, it is noteworthy that the binding site for **7t** in this structure and the known binding site for **1** are connected through a long, flexible loop, which may provide a mechanism for linking these two sites.

We have previously reported the structure of a noncooperative fragment, an indole glyoxylate, also tethered at Y31C [PDB entry 1M4A (*34*)]. Figure 8B shows the structure of the indole glyoxylate superimposed on the structure of **7t** tethered to Y31C-IL-2. The residues surrounding the indole (K35, R38, L72, and A73) are the same as those surrounding the distal ring of **1** (Figure 2). Thus, while the indole glyoxylate and the carboline fragments can be covalently attached to IL-2 at the same residue, they bind in nonoverlapping sites. Interestingly, these sites coincide with the binding sites for two chains of the IL-2 receptor (*30*−*33*). By performing tethering selections under different conditions, we were able to identify two, biologically relevant binding sites for fragments within the adaptive region of IL-2. Far from being intractable for small-molecule discovery, IL-2 is highly prone to binding small, organic ligands.

CONCLUSION

Tethering in the presence of a known antagonist has led to the identification of a new binding site for small molecules in the dynamic region of IL-2. These two sites can bind ligands cooperatively, gaining as much at −2 kcal/mol in the free energy of binding. This strong cooperativity could result from direct interactions between the ligands and/or through conformational changes in the adaptive region. X-ray crystallography suggests that cooperativity may be mediated by conformational changes in the loop bridging the two binding sites, but a direct interaction between ligands may also be important. Crystallography also demonstrates that there are distinct small-molecule binding sites in IL-2, a discovery that may lead to the development of tight-binding inhibitors for this important immunomodulator.

Tethering has proven to be an efficient and informative method for discovering ligands for IL-2. As a screening method, tethering is rapid and uses only single-milligram quantities of protein. Because the method is site-selective, it is possible to focus the fragment discovery effort in the adaptive region of IL-2. The covalent tether is then used to affix one member of the cooperative pair of ligands to the protein, allowing a number of mechanistic experiments to be performed, in both tethering and SPR contexts. Finally, tethering facilitates X-ray crystallography, making it possible to structurally characterize the fragment **7t** bound to IL-2. The tethering experiments described here provide a new, site-selective approach to discovering and characterizing cooperatively binding ligands in adjacent sites. Moreover, experiments with IL-2 suggest that focusing on dynamic regions of protein structure holds promise for the development of small-molecule antagonists of a protein−protein interaction.

ACKNOWLEDGMENT

We thank S. White, M. Bui, and J. Jacobs for synthesis of fragments for tethering and SPR and J. Wang for preparation of Y31C/K43C-IL-2.

REFERENCES

1. Luque, I., and Freire, E. (2000) *Proteins* (Suppl.), 63−71.
2. Ma, B., Shatsky, M., Wolfson, H. J., and Nussinov, R. (2002) *Protein Sci. 11*, 184−197.
3. Bursavich, M. G., and Rich, D. H. (2002) *J. Med. Chem. 45*, 541−558.
4. Rockwell, A., Melden, M., Copeland, R. A., Hardman, K., Decicco, C. P., and DeGrado, W. F. (1996) *J. Am. Chem. Soc. 118*, 10337−10338.

5. Stout, T. J., Tondi, D., Rinaldi, M., Barlocco, D., Pecorari, P., Santi, D. V., Kuntz, I. D., Stroud, R. M., Shoichet, B. K., and Costi, M. P. (1999) *Biochemistry 38*, 1607−1617.
6. Fritz, T. A., Tondi, D., Finer-Moore, J. S., Costi, M. P., and Stroud, R. M. (2001) *Chem. Biol. 8*, 981−995.
7. McCallum, S. A., Hitchens, T. K., Torborg, C., and Rule, G. S. (2000) *Biochemistry 39*, 7343−7356.
8. Lugovskoy, A. A., Degterev, A. I., Fahmy, A. F., Zhou, P., Gross, J. D., Yuan, J., and Wagner, G. (2002) *J. Am. Chem. Soc. 124*, 1234−1240.
9. Schindler, T., Bornmann, W., Pellicena, P., Miller, W. T., Clarkson, B., and Kuriyan, J. (2000) *Science 289*, 1938−1942.
10. Pargellis, C., Tong, L., Churchill, L., Cirillo, P. F., Gilmore, T., Graham, A. G., Grob, P. M., Hickey, E. R., Moss, N., Pav, S., and Regan, J. (2002) *Nat. Struct. Biol. 9*, 268−272.
11. Livnah, O., Stura, E. A., Johnson, D. L., Middleton, S. A., Mulcahy, L. S., Wrighton, N. C., Dower, W. J., Jolliffe, L. K., and Wilson, I. A. (1996) *Science 273*, 464−471.
12. DeLano, W. L., Ultsch, M. H., de Vos, A. M., and Wells, J. A. (2000) *Science 287*, 1279−1283.
13. Sundberg, E. J., and Mariuzza, R. A. (2000) *Struct. Folding Des. 8*, R137−R142.
14. Cochran, A. G. (2000) *Chem. Biol. 7*, R85−R94.
15. Way, J. C. (2000) *Curr. Opin. Chem. Biol. 4*, 40−46.
16. Cochran, A. G. (2001) *Curr. Opin. Chem. Biol. 5*, 654−659.
17. Toogood, P. L. (2002) *J. Med. Chem. 45*, 1−16.
18. Huang, Z. (2002) *Chem. Biol. 9*, 1059−1072.
19. Gadek, T. R., and Nicholas, J. B. (2003) *Biochem. Pharmacol. 65*, 1−8.
20. Hajduk, P. J., Meadows, R. P., and Fesik, S. W. (1999) *Q. Rev. Biophys. 32*, 211−240.
21. Ramstrom, O., and Lehn, J.-M. (2002) *Nat. Rev. Drug Discovery 1*, 26−36.
22. Erlanson, D. A., Braisted, A. C., Raphael, D. R., Randal, M., Stroud, R. M., Gordon, E. M., and Wells, J. A. (2000) *Proc. Natl. Acad. Sci. U.S.A. 97*, 9367−9372.
23. Erlanson, D. A., Lam, J., Wiesmann, C., Luong, T., Simmons, B., DeLano, W., Choong, I. C., Burdett, M. T., Flanagan, M., Lee, D., Gordon, E. M., and O'Brien, T. (2003) *Nat. Biotechnol. 21*, 308−314.
24. Olejniczak, E. T., Hajduk, P. J., Marcotte, P. A., Nettesheim, D. G., Meadows, R. P., Edalji, R., Holzman, T. F., and Fesik, S. W. (1997) *J. Am. Chem. Soc. 119*, 5828−5832.
25. Nelson, B. H., and Willerford, D. M. (1998) *Adv. Immunol. 70*, 1−81.
26. Waldmann, T. A., and O'Shea, J. (1998) *Curr. Opin. Immunol. 10*, 507−512.
27. Berard, J. L., Velez, R. L., Freeman, R. B., and Tsunoda, S. M. (1999) *Pharmacotherapy 19*, 1127−1137.
28. Brok, H. P., Tekoppele, J. M., Hakimi, J., Kerwin, J. A., Nijenhuis, E. M., De Groot, C. W., Bontrop, R. E., and Hart, B. A. (2001) *Clin. Exp. Immunol. 124*, 134−141.
29. Carswell, C. I., Plosker, G. L., and Wagstaff, A. J. (2001) *BioDrugs 15*, 745−773.
30. Wang, Z., Zheng, Z., Sun, L., and Liu, X. (1995) *Eur. J. Immunol. 25*, 1212−1216.
31. Zurawski, S. M., Vega, F., Jr., Doyle, E. L., Huyghe, B., Flaherty, K., McKay, D. B., and Zurawski, G. (1993) *EMBO J. 12*, 5113−5119.
32. Sauve, K., Nachman, M., Spence, C., Bailon, P., Campbell, E., Tsien, W. H., Kondas, J. A., Hakimi, J., and Ju, G. (1991) *Proc. Natl. Acad. Sci. U.S.A. 88*, 4636−4640.
33. Weigel, U., Meyer, M., and Sebald, W. (1989) *Eur. J. Biochem. 180*, 295−300.
34. Arkin, M. R., Mike, R., Delano, W. L., Hyde, J., Luong, T. N., Oslob, J. D., Raphael, D. R., Taylor, L., Wang, J., McDowell, R. S., Wells, J. A., and Braisted, A. C. (2003) *Proc. Natl. Acad. Sci. U.S.A. 100*, 1603−1608.
35. Tilley, J. W., Chen, L., Fry, D. C., Emerson, S. D., Powers, G. D., Biondi, D., Varnell, T., Trilles, R., Guthrie, R., Mennona, F., Kaplan, G., LeMahieu, R. A., Carson, M., Han, R.-J., Liu, C.-M., Palermo, R., and Ju, G. (1997) *J. Am. Chem. Soc. 119*, 7589−7590.
36. Pflugrath, J. W. (1999) *Acta Crystallogr. D55*, 1718−1725.
37. Collaborative Computational Project Number 4 (1994) *Acta Crystallogr. D55*, 1718−1725.
38. Jones, T. A., Zou, J. Y., Cowan, S. W., and Kjeldgaard, M. (1991) *Acta Crystallogr. A47*, 110−119.
39. Forsen, S., and Linse, S. (1995) *Trends Biochem. Sci. 20*, 495−497.
40. McKay, D. B. (1992) *Science 257*, 412−413.
41. Mott, H. R., Baines, B. S., Hall, R. M., Cooke, R. M., Driscoll, P. C., Weir, M. P., and Campbell, I. D. (1995) *J. Mol. Biol. 247*, 979−994.

BI034138G